

ΛNN content of Λ -nucleus potential

Eliahu Friedman^{1,*} and Avraham Gal^{1,**}

¹Racah Institute of Physics, The Hebrew University, Jerusalem 9190401, Israel

Abstract. A minimally constructed Λ -nucleus density-dependent optical potential is used to calculate binding energies of observed $1s_\Lambda$, $1p_\Lambda$ states across the periodic table, leading to a repulsive ΛNN contribution $D_\Lambda^{(3)} \approx 14$ MeV to the phenomenological Λ -nucleus potential depth $D_\Lambda \approx -30$ MeV. This value is significant in connection with the so-called ‘hyperon puzzle.’

1 Introduction

The Λ -nucleus potential depth provides an important constraint in ongoing attempts to resolve the ‘hyperon puzzle’, i.e., whether or not dense neutron-star matter contains hyperons, primarily Λ s besides nucleons [1]. Figure 1 presents compilation of most of the known Λ hypernuclear binding energies (B_Λ) across the periodic table, fitted by a three-parameter Woods-Saxon (WS) attractive potential. As $A \rightarrow \infty$, a limiting value of $B_\Lambda(A) \rightarrow 30$ MeV is obtained. Interestingly, studies of density dependent Λ -nuclear optical potentials $V_\Lambda(\rho)$ in Ref. [2], with ρ the nuclear density normalized to the number of nucleons A , conclude that a ρ^2 term motivated by three-body ΛNN interactions provides a large repulsive (positive) contribution to the Λ -nuclear potential depth D_Λ at nuclear-matter density ρ_0 : $D_\Lambda^{(3)} \approx 30$ MeV. This repulsive component of D_Λ is more than just compensated at ρ_0 by a roughly twice larger attractive depth value $D_\Lambda^{(2)} \approx -60$ MeV, motivated by a two-body ΛN interaction. Note that D_Λ is defined as $V_\Lambda(\rho_0)$ in the limit $A \rightarrow \infty$ at a given nuclear-matter density ρ_0 , with a value 0.17 fm^{-3} assumed here.

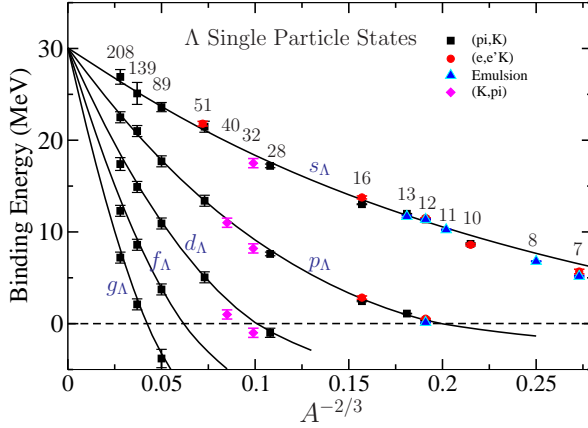
Most hyperon-nucleon potential models overbind Λ hypernuclei, yielding values of $D_\Lambda^{(2)}$ deeper than -30 MeV. Whereas such overbinding amounts to only few MeV in the often used Nijmegen soft-core model versions NSC97e,f [4] it is considerably stronger, by more than 10 MeV, in the recent Nijmegen extended soft-core model ESC16 [5]. A similar overbinding arises at leading order in chiral effective field theory (χ EFT) [6]. The situation at next-to leading order (NLO) is less clear owing to a strong dependence of $D_\Lambda^{(2)}$ on the momentum cutoff scale λ [7]. At $\lambda=500$ MeV/c, however, it is found in Ref. [8] that both versions NLO13 [9] and NLO19 [10] overbind by a few MeV. Finally, recent Quantum Monte Carlo (QMC) calculations [11, 12], using a $\Lambda N + \Lambda NN$ interaction model designed to bind correctly ${}^5_\Lambda\text{He}$, result in a strongly attractive $D_\Lambda^{(2)}$ of order -100 MeV and a correspondingly large repulsive (positive) $D_\Lambda^{(3)}$, reproducing the overall potential depth $D_\Lambda \approx -30$ MeV.

Our aim in the present phenomenological study is to check to what extent properly chosen Λ hypernuclear binding energy data, with *minimal* extra assumptions, imply positive values of $D_\Lambda^{(3)}$, and

*Eliahu.Friedman@mail.huji.ac.il

**avragal@savion.huji.ac.il

Update: Millener, Dover, Gal PRC 38, 2700 (1988)



Woods-Saxon $V = 30.05$ MeV, $r = 1.165$ fm, $a = 0.6$ fm

Figure 1. Compilation of Λ binding energies in ${}^7\text{Li}$ to ${}^{208}\text{Pb}$ from various sources, and as calculated using a three-parameter WS potential [2]. Figure adapted from Ref. [3]

how large it is [13]. Repulsive three-body ΛNN interactions go beyond just providing solution of the overbinding problem: as nuclear density is increased beyond nuclear matter density ρ_0 , the balance between attractive $D_\Lambda^{(2)}$ and repulsive $D_\Lambda^{(3)}$ tilts towards the latter. This results in nearly total expulsion of Λ hyperons from neutron-star matter, suggesting an equation of state (EoS) sufficiently stiff to support two solar-mass neutron stars, thereby providing a possible solution to the ‘hyperon puzzle’. The larger $D_\Lambda^{(3)}$ is, the more likely it is a solution [14, 15]. However, there is no guarantee that three-body ΛNN interactions are universally repulsive. For a recent discussion of this problem within an $SU(3)$ ‘decuplet dominance’ approach practised in modern χ EFT studies at NLO, see Ref. [8].

In this Contribution we adopt the optical potential approach as applied by Dover-Hüfner-Lemmer to pions in nuclear matter [16]. For the Λ -nucleus system, it provides expansion in powers of the nuclear density $\rho(r)$, consisting of a linear term induced by a two-body ΛN interaction plus two higher-power density terms: (i) a long-range Pauli correlations term starting at $\rho^{4/3}$, and (ii) a short-range ΛNN interaction term dominated in the present context by three-body ΛNN interactions, starting at ρ^2 . As demonstrated below, the contribution of the Pauli correlations term is non negligible, propagating to higher powers of density terms than just $\rho^{4/3}$, such as the ρ^2 ΛNN interaction term. This explains why the value derived here, $D_\Lambda^{(3)} = (13.9 \pm 1.4)$ MeV, differs from any of those suggested earlier in Ref. [2] and in Skyrme Hartree Fock studies [17] where Pauli correlations are usually disregarded. Our value of $D_\Lambda^{(3)}$ strongly disagrees with the much larger value inferred in QMC calculations [12]. We comment on these discrepancies below.

2 Nuclear densities

In optical model applications aimed at establishing relations between components with different powers of density $\rho = \rho_p + \rho_n$, it is crucial to ensure that the radial extent of the densities, e.g., their r.m.s.

radii, follows closely values derived from experiment. For proton densities we used charge densities, with proton finite-size and recoil effects included. Harmonic-oscillator type densities [18] were used for the lightest elements, assuming the same radial parameters for protons and neutrons. A variation of 1% in the r.m.s. neutron radius was found to affect calculated Λ binding energies considerably less than given by most of the experimental uncertainties listed in Table 1 below. For a detailed discussion in the analogous case of light Ξ^- hypernuclei, see Ref. [19]. For species beyond the nuclear $1p$ shell we used two-parameter Fermi distributions normalized to Z for protons and $N = A - Z$ for neutrons, derived from assembled nuclear charge distributions [20]. For medium-weight and heavy nuclei, the r.m.s. radii of our neutron density distributions assume larger values than those for proton density distributions, as practiced in analyses of exotic atoms [21]. Furthermore, once neutron orbits extend beyond proton orbits, it is useful to represent the nuclear density $\rho(r)$ as

$$\rho(r) = \rho_{\text{core}}(r) + \rho_{\text{excess}}(r), \quad (1)$$

where ρ_{core} refers to the Z protons plus the charge symmetric Z neutrons occupying the same nuclear ‘core’ orbits, and ρ_{excess} refers to the $(N - Z)$ ‘excess’ neutrons associated with the nuclear periphery.

3 Optical potential

The optical potential employed in this work, $V_{\Lambda}^{\text{opt}}(\rho) = V_{\Lambda}^{(2)}(\rho) + V_{\Lambda}^{(3)}(\rho)$, consists of terms representing two-body ΛN and three-body ΛNN interactions, respectively:

$$V_{\Lambda}^{(2)}(\rho) = -\frac{4\pi}{2\mu_{\Lambda}} f_A C_{\text{Pauli}}(\rho) b_0 \rho, \quad (2)$$

$$V_{\Lambda}^{(3)}(\rho) = +\frac{4\pi}{2\mu_{\Lambda}} f_A B_0 \frac{\rho^2}{\rho_0}, \quad (3)$$

with b_0 and B_0 strength parameters in units of fm ($\hbar = c = 1$). In these expressions, $\rho(r)$ is a nuclear density distribution normalized to the number of nucleons A , $\rho_0 = 0.17 \text{ fm}^{-3}$ stands for nuclear-matter density, μ_{Λ} is the Λ -nucleus reduced mass and f_A is a kinematical factor transforming b_0 from the ΛN c.m. system to the Λ -nucleus c.m. system:

$$f_A = 1 + \frac{A-1}{A} \frac{\mu_{\Lambda}}{m_N}. \quad (4)$$

This form of f_A coincides with the way it is used for $V_{\Lambda}^{(2)}$ in atomic/nuclear hadron-nucleus bound-state problems [21] and its A dependence provides good approximation for $V_{\Lambda}^{(3)}$. Next is the density dependent factor $C_{\text{Pauli}}(\rho)$ in Eq. (2), standing for a Pauli correlation function:

$$C_{\text{Pauli}}(\rho) = (1 + \alpha_P \frac{3k_F}{2\pi} f_A b_0)^{-1}, \quad (5)$$

with Fermi momentum $k_F = (3\pi^2\rho/2)^{1/3}$. The parameter α_P in Eq. (5) switches off ($\alpha_P=0$) or on ($\alpha_P=1$) Pauli correlations in a form suggested in Ref. [22] and practised in K^- atoms studies [23]. To estimate $1/A$ correction terms, we also approximated $C_{\text{Pauli}}(\rho)$ by [19]:

$$C_{\text{Pauli}}(\rho) \approx (1 + \alpha_P \frac{3k_F}{2\pi} b_0^{\text{lab}})^{-1}, \quad b_0^{\text{lab}} = (1 + \frac{m_{\Lambda}}{m_N}) b_0. \quad (6)$$

As shown below, including $C_{\text{Pauli}}(\rho)$ in $V_{\Lambda}^{(2)}$ affects strongly the balance between the derived potential depths $D_{\Lambda}^{(2)}$ and $D_{\Lambda}^{(3)}$. However, introducing it also in $V_{\Lambda}^{(3)}$ is found to make little difference, which is why it is skipped in Eq. (3). Finally we note that the low-density limit of V_{Λ}^{opt} requires according to Ref. [16] that b_0 is identified with the c.m. ΛN spin-averaged scattering length (positive here).

4 Data

Table 1. Binding energies in MeV, including uncertainties, considered here; taken from Table IV of Ref. [3].

hypernucleus	$1s_\Lambda$	\pm	$1p_\Lambda$	\pm
$^{12}_\Lambda\text{B}$	11.52	0.02	0.54	0.04
$^{13}_\Lambda\text{C}$	12.0	0.2	1.1	0.2
$^{16}_\Lambda\text{N}$	13.76	0.16	2.84	0.18
$^{28}_\Lambda\text{Si}$	17.2	0.2	7.6	0.2
$^{32}_\Lambda\text{S}$	17.5	0.5	8.2	0.5
$^{51}_\Lambda\text{V}$	21.5	0.6	13.4	0.6
$^{89}_\Lambda\text{Y}$	23.6	0.5	17.7	0.6
$^{139}_\Lambda\text{La}$	25.1	1.2	21.0	0.6
$^{208}_\Lambda\text{Pb}$	26.9	0.8	22.5	0.6

The present work does not attempt to reproduce the full range of B_Λ data shown in Fig. 1. It is limited to $1s_\Lambda$ and $1p_\Lambda$ states listed in Table 1. We fit to such states in *one* of the nuclear $1p$ -shell hypernuclei listed in the table, where the $1s_\Lambda$ state is bound by over 10 MeV while the $1p_\Lambda$ state has just become bound. This helps resolve the density dependence of V_Λ^{opt} by setting a good balance between its two components, $V_\Lambda^{(2)}(\rho)$ and $V_\Lambda^{(3)}(\rho)$, following it all the way to $^{208}_\Lambda\text{Pb}$ the heaviest hypernucleus marked in Fig. 1. We chose to fit the $^{16}_\Lambda\text{N}$ precise $B_\Lambda^{\text{exp}}(1s, 1p)$ values derived, respectively, from the first and third peaks to the left in Fig. 2. The extremely simple $1p$ proton hole structure of the ^{15}N nuclear core in this case removes most of the uncertainty arising from spin-dependent residual ΛN interactions [25]. The fitted optical-potential parameters b_0 , Eq. (2), and B_0 , Eq. (3), are then used to calculate the $B_\Lambda^{1s,1p}$ values of the other eight species listed in Table 1.

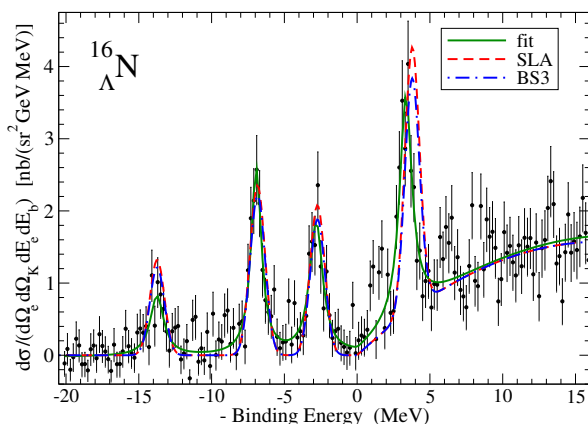


Figure 2. $^{16}\text{O}(e, e'K^+)$ spectrum of $^{16}_\Lambda\text{N}$ from JLab Hall A measurements. Figure adapted from Ref. [24].

5 Results

The two strength parameters b_0, B_0 of the optical potential terms Eqs. (2,3) were obtained by fitting to the ${}^{16}_\Lambda\text{N } B_\Lambda^{\text{exp}}(1s, 1p)$ values listed in Table 1. Suppressing Pauli correlations by setting $\alpha_p = 0$ in Eqs. (5,6), the resulting Λ potential depth $D_\Lambda = -27.4$ MeV reflects a sizable cancellation between a strongly attractive two-body potential depth $D_\Lambda^{(2)}$ and a strongly repulsive three-body potential depth $D_\Lambda^{(3)}$. The overall agreement between calculations and experiment is acceptable, but some underbinding appears to develop for increasing mass numbers A , noticed clearly in the three heaviest $1s_\Lambda$ and two heaviest $1p_\Lambda$ states. The resulting b_0 is about half of the known Λp scattering length of (1.7 ± 0.1) fm [26, 27].

When the full potential Eqs. (2-6) is used (marked here as model X, including Pauli correlations through $\alpha_p = 1$) the overall picture remains unchanged regarding underbinding for the heavier elements, see Fig. 3. However, the fit parameter $b_0=1.85$ fm agrees now with the Λp scattering length. The other parameter, $B_0 = 0.170$ fm, is about twice smaller than for $\alpha_p = 0$.

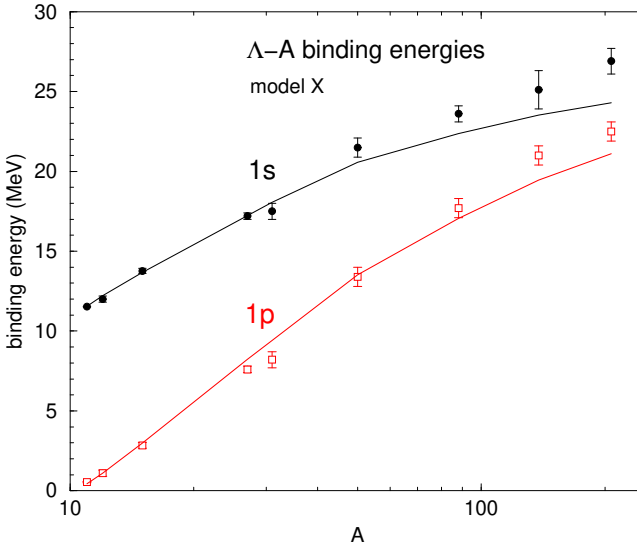


Figure 3. $B_\Lambda^{1s,1p}(A)$ values from model X compared with data. Continuous lines connect calculated values.

The phenomenon of underbinding associated with the optical potential Eqs. (2-6) is likely to be a result of the use of ρ^2 in nuclei where excess neutrons occupy shell-model orbits higher than those occupied by protons. This situation occurs in Fig. 3 for the four hypernuclei with $A \gtrsim 50$. Expecting that direct three-body ΛNN contributions involving one ‘core’ nucleon and one ‘excess’ nucleon vanish upon summing on the $T=0$ ‘core’ closed-shell nucleons, we modify $\rho^2 = (\rho_{\text{core}} + \rho_{\text{excess}})^2$ by discarding the bilinear term $\rho_{\text{core}} \rho_{\text{excess}}$, thereby replacing ρ^2 in $V_\Lambda^{(3)}$, Eq. (3), by

$$\rho_{\text{core}}^2 + \rho_{\text{excess}}^2 = (2\rho_p)^2 + (\rho_n - \rho_p)^2 \quad (7)$$

in terms of the input densities ρ_p and ρ_n . This ansatz is consistent with an overall isospin factor $\tau_1 \cdot \tau_2$ in two-pion exchange ΛNN forces, as first realized back in 1958 [28]. Results of applying this ansatz are shown in the lower part of Fig. 4 as model Y, where the underbinding of calculated $1s_\Lambda$ and

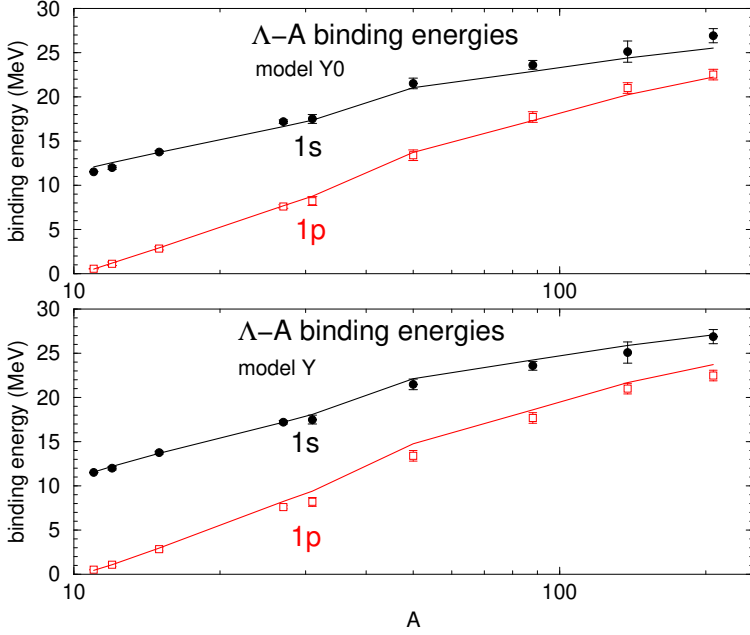


Figure 4. $B_{\Lambda}^{1s,1p}(A)$ values from models Y0 and Y compared with data, see text. Continuous lines connect calculated values.

$1p_{\Lambda}$ binding energies noticed in model X is no longer observed. The fit parameters, nevertheless, are the same as for model X above. In the upper part of Fig. 4, model Y0 shows similar results where the Pauli-correlations correction in model Y, Eq. (6), is replaced by Eq. (5). This provides a rough estimate of the impact of $1/A$ corrections typical for our optical-potential methodology. Potential depth values in model Y are $D_{\Lambda}^{(2)} = -41.6$ MeV, $D_{\Lambda}^{(3)} = 13.9$ MeV.

To estimate uncertainties, we act as follows: (i) decreasing the input value of $B_{\Lambda}^{1s}(^{16}_{\Lambda}\text{N})$ fitted to by 0.2 MeV, thereby getting halfway to the central value of $B_{\Lambda}^{1s}(^{16}_{\Lambda}\text{O}) = (13.4 \pm 0.4)$ MeV for $^{16}_{\Lambda}\text{O}$ [29] the charge-symmetric partner of $^{16}_{\Lambda}\text{N}$, results in approximately 10% larger value of $D_{\Lambda}^{(3)}$, and (ii) applying Pauli correlations to $V_{\Lambda}^{(3)}$ too reduces $D_{\Lambda}^{(3)}$ roughly by 10%. In both cases $D_{\Lambda}^{(2)}$ increases moderately by $\lesssim 1$ MeV. On the other hand, $D_{\Lambda}^{(2)}$ decreases by 1.7 MeV if Eq. (5) is used for $C_{\text{Pauli}}(\rho)$ instead of Eq. (6). Considering these uncertainties, our final values are (in MeV)

$$D_{\Lambda}^{(2)} = -40.6 \pm 1.0 \quad D_{\Lambda}^{(3)} = 13.9 \pm 1.4 \quad D_{\Lambda} = -26.7 \pm 1.7 \quad (8)$$

6 Discussion

The $D_{\Lambda}^{(2)}$ and $D_{\Lambda}^{(3)}$ values in Eq. (8) are considerably smaller than those deduced in QMC calculations [11, 12]. Note that the QMC nuclear densities $\rho_{\text{QMC}}(r)$ are much too compact with respect to our realistic densities, with nuclear r.m.s. radii $r_N(\text{QMC})$ about 0.8 of the known r.m.s. charge radii in ^{16}O and ^{40}Ca [30]. Since ρ scales as r_N^{-3} , applying it to the density dependence of our V_{Λ}^{opt} would transform $D_{\Lambda}^{(2)}$ and $D_{\Lambda}^{(3)}$ of Eq. (8) to as large depth values as $D_{\Lambda}^{(2)}(\text{QMC}) = (-79.3 \pm 2.0)$ MeV and

$D_{\Lambda}^{(3)}(\text{QMC})=(53.0\pm 5.3)$ MeV, their sum $D_{\Lambda}(\text{QMC})=(-26.3\pm 5.7)$ MeV agreeing within uncertainties with ours.

Table 2. Λ -nuclear potential depths (in MeV) from two SHF calculations fitting B_{Λ} data points, and from our own $V_{\Lambda}^{\text{opt}}(\alpha_P = 0)$ two-parameter (b_0, B_0) fit to the two $B_{\Lambda}^{1s,1p}(^{16}_{\Lambda}\text{N})$ values listed in Table 1.

Method	Data Points	$D_{\Lambda}^{(2)}$	$D_{\Lambda}^{(3)}$	D_{Λ}
SHF [2]	3	-57.8	31.4	-26.4
SHF [17]	35	-55.4	20.4	-35.0
$V_{\Lambda}^{\text{opt}}(\alpha_P = 0)$ [13]	2	-57.6	30.2	-27.4

Smaller-size but still inflated values of $D_{\Lambda}^{(2)}$ and $D_{\Lambda}^{(3)}$ are obtained by applying the Skyrme Hartree Fock (SHF) methodology [2, 17]. Apart from small nonlocal potential terms and effective mass corrections, the SHF Λ -nuclear mean-field potential $V_{\Lambda}(\rho)$ consists of two terms: $V_{\Lambda}^{(2)}(\rho) \propto \rho$ and $V_{\Lambda}^{(3)}(\rho) \propto \rho^2$. A large-scale SHF fit [17] of the corresponding Λ potential depths to 35 B_{Λ} data points is listed in the middle row of Table 2. We note that the overall $D_{\Lambda} = -35$ MeV value becomes -31 MeV upon including a Λ effective-mass correction, a bit closer to the other D_{Λ} values listed in the table. Similar results, particularly for $D_{\Lambda}^{(2)}$, can be obtained in fact by choosing a considerably smaller number of fitted data points, as shown by the fits listed in the other two rows of the table. The 11 MeV difference between the $D_{\Lambda}^{(3)}$ values derived in these two SHF calculations arises mostly from nonlocal lower-power density terms, like $\rho^{5/3}$, present in [17] but absent in [2]. Interestingly, the last row lists a fit to the two $B_{\Lambda}^{1s,1p}(^{16}_{\Lambda}\text{N})$ values used here when Pauli correlations are suppressed, $\alpha_P = 0$ in Eq. (5). The sizable difference between $D_{\Lambda}^{(2)}$ and $D_{\Lambda}^{(3)}$ values listed in Table 2, all of which disregard Pauli correlations, and the V_{Λ}^{opt} values listed in Eq. (8) demonstrates the importance of including in V_{Λ}^{opt} a Pauli-correlations term ($\alpha_P = 1$) starting as $\rho^{4/3}$.

7 Summary

In summary, we have presented a straightforward optical-potential analysis of $1s_{\Lambda}$ and $1p_{\Lambda}$ binding energies across the periodic table, $12 \leq A \leq 208$, based on nuclear densities constrained by charge r.m.s. radii. The potential is parameterized by constants b_0 and B_0 in front of two-body ΛN and three-body ΛNN interaction terms. These parameters were fitted to precise $B_{\Lambda}^{\text{exp}}(1s, 1p)$ values in $^{16}_{\Lambda}\text{N}$ [31] and then used to evaluate $B_{\Lambda}^{1s,1p}$ values in the other hypernuclei considered here. Pauli correlations were found essential to establish a correct balance between b_0 and B_0 , as judged by b_0 coming out in the final model Y analysis close to the value of the ΛN spin-averaged s -wave scattering length. Good agreement was reached in this model between the calculated $B_{\Lambda}^{1s,1p}$ values and their corresponding B_{Λ}^{exp} values, see Fig. 4.

The potential depth $D_{\Lambda}^{(3)}$ derived here, Eq. (8), suggests that in symmetric nuclear matter the Λ -nucleus potential becomes repulsive near three times ρ_0 . Our derived depth $D_{\Lambda}^{(3)}$ is larger by a few MeV than the one yielding $\mu(\Lambda) > \mu(n)$ for Λ and neutron chemical potentials in purely neutron matter, respectively, under a ‘decuplet dominance’ construction for the underlying ΛNN interaction terms within a $\chi\text{EFT(NLO)}$ model [8]. This suggests that the strength of the corresponding repulsive $V_{\Lambda}^{(3)}$ optical potential component, as constrained in the present work by data, is sufficient to prevent Λ hyperons from playing active role in neutron-star matter, thereby enabling a stiff EoS that supports two solar-mass neutron stars.

Acknowledgments

One of us (A.G.) thanks Jiří Mareš and other members of the HYP2022 organizing team for their generous hospitality during the Conference. The present work is part of a project funded by the European Union's Horizon 2020 research & innovation programme, grant agreement 824093.

References

- [1] L. Tolos, L. Fabbietti, Prog. Part. Nucl. Phys. **112**, 103770 (2020), and past neutron-star work cited therein
- [2] D.J. Millener, C.B. Dover, A. Gal, Phys. Rev. C **38**, 2700 (1988)
- [3] A. Gal, E.V. Hungerford, D.J. Millener, Rev. Mod. Phys. **88**, 035004 (2016)
- [4] Th.A. Rijken, V.G.J. Stoks, Y. Yamamoto, Phys. Rev. C **59**, 21 (1999)
- [5] M.M. Nagels, Th.A. Rijken, Y. Yamamoto, Phys. Rev. C **99**, 044003 (2019)
- [6] H. Polinder, J. Haidenbauer, U.-G. Meißner, Nucl. Phys. A **779**, 244 (2006)
- [7] J. Haidenbauer, I. Vidaña, Eur. Phys. J. A **56**, 55 (2020)
- [8] D. Gerstung, N. Kaiser, W. Weise, Eur. Phys. J. A **56**, 175 (2020), and references cited therein to earlier works on ΛNN interactions in χ EFT.
- [9] J. Haidenbauer, S. Petschauer, N. Kaiser, U.-G. Meißner, A. Nogga, W. Weise, Nucl. Phys. A **915**, 24 (2013)
- [10] J. Haidenbauer, U.-G. Meißner, A. Nogga, Eur. Phys. J. A **56**, 91 (2020)
- [11] D. Lonardoni, S. Gandolfi, F. Pederiva, Phys. Rev. C **87**, 041303(R) (2013)
- [12] D. Lonardoni, F. Pederiva, S. Gandolfi, Phys. Rev. C **89**, 014314 (2014)
- [13] E. Friedman, A. Gal, Phys. Lett. B **837**, 137669 (2023)
- [14] D. Lonardoni, A. Lovato, S. Gandolfi, F. Pederiva, Phys. Rev. Lett. **114**, 092301 (2015)
- [15] D. Logoteta, I. Vidaña, I. Bombaci, Eur. Phys. J. A **55**, 207 (2019)
- [16] C.B. Dover, J. Hüfner, R.H. Lemmer, Ann. Phys. (NY) **66**, 248 (1971)
- [17] H.-J. Schulze, E. Hiyama, Phys. Rev. C **90**, 047301 (2014), and past SHF work cited therein
- [18] L.R.B. Elton, Nuclear Sizes (Oxford University Press, Oxford, 1961)
- [19] E. Friedman, A. Gal, Phys. Lett. B **820**, 136555 (2021)
- [20] I. Angeli, K.P. Marinova, At. Data Nucl. Data Tables **99**, 69 (2013)
- [21] E. Friedman, A. Gal, Phys. Rep. **452**, 89 (2007)
- [22] T. Waas, M. Rho, W. Weise, Nucl. Phys. A **617**, 449 (1997)
- [23] E. Friedman, A. Gal, Nucl. Phys. A **959**, 66 (2017), and past K^- atoms work cited therein
- [24] F. Garibaldi, *et al.* (Jefferson Lab Hall A Collaboration), Phys. Rev. C **99**, 054309 (2019)
- [25] D.J. Millener, Nucl. Phys. A **804**, 84 (2008), **881**, 298 (2012), **914**, 109 (2013)
- [26] G. Alexander, *et al.*, Phys. Rev. **173**, 1452 (1968)
- [27] A. Budzanowski, *et al.* (HIRES Collaboration), Phys. Lett. B **687**, 31 (2010)
- [28] R. Spitzer, Phys. Rev. **110**, 1190 (1958)
- [29] M. Agnello, *et al.* (FINUDA Collaboration), Phys. Lett. B **698**, 219 (2011)
- [30] D. Lonardoni, Ph.D. thesis, University of Trento, Italy, arXiv:1311.6672 [nucl-th], in particular see Table 4.7
- [31] F. Cusanno, *et al.* (Jefferson Lab Hall A Collaboration), Phys. Rev. Lett. **103**, 202501 (2009)